NBSIR 82-2569(R)
Div. 561

HIGH TEMPERATURE APPLICATIONS OF STRUCTURAL CERAMICS

QUARTERLY PROGRESS REPORT

April - June 1982

Samuel J. Schneider
Project Manager

Center for Materials Science
National Bureau of Standards
U. S. Department of Commerce
Washington, D. C. 20234

PREPARED FOR THE UNITED STATES
DEPARTMENT OF ENERGY

Under Contract No. DE-A105-800R20679

TABLE OF CONTENTS

NBS-5.12 - HIGH TEMPERATURE APPLICATIONS OF STRUCTURAL CERAMICS

E. R. Fuller, R. J. Fields, T. J. Chuang,
R. Krause, A. Dragoo and S. J. Schneider

National Bureau of Standards
Center for Materials Science
Washington, D. C. 20234

INTRODUCTION

The achievement of higher efficiency thermochemical engines and heat recovery systems requires the availability of high temperature, high performance structural materials. Structural ceramics such as SiC, Si_3N_4 and certain Al_2O_3-Si_3N_4 combinations have received particular attention for these applications due to their basic characteristics of good strengths coupled with good corrosion and thermal shock resistances. Even with these positive attributes, improved reliabilities and extended lifetimes under service conditions are necessary for structural ceramics to gain industrial acceptance and use. The problems are mechanical and/or chemical in nature and are enhanced by the fact that these materials are subjected to high temperatures, reactive environments and extreme thermal gradients.

With an objective of improved performance for heat engine/heat recovery applications the NBS program on structural ceramics addresses these problems through the determination of the critical factors which influence mechanical and microstructural behavior. The activities of the program are grouped under four major subtasks with each designed to develop key data, associated test methods and companion predictive models. The status of the subtasks are detailed in the following sections.

NBS-5.12(A) - HIGH TEMPERATURE FRACTURE OF STRUCTURAL CERAMICS

DISCUSSION OF CURRENT ACTIVITIES

Chevron-notched beam specimens of NC-430 were fractured under four-point bending for a range of loading rates from 0.0002 in/min to 0.02 in/min and temperatures from RT to 1350 °C. The majority of the specimens were found to fail in transgranular mode.

Table I lists the raw data obtained for fracture toughness (K_{IC}) determination. Note that the K_{IC} values in the last column of the table are only preliminary results derived from the K_{IC} expression using peak load and minimum Y (K_{IC} = Pmax Y). True K_{IC} values must wait until SEM work is done so that the actual crack length at which fast fracture occurs can be determined.

Two figures can be derived from Table I. Figure 1 shows K_{IC} vs. T plot for several loading rates. The data indicates K_{IC} increases when T increases. This result is consistent with test data obtained from other ceramic materials. It is thought that creep deformation near the crack tip might be responsible for this effect.

Figure 2 demonstrates K_{IC} versus $\dot{\delta}$ at various temperatures. The data at 1350 °C show a linear decrease of K_{IC} as $\dot{\delta}$ increases on a semi-log scale. It is believed that crack tip blunting may play a role in the increase of K_{IC} especially in the low $\dot{\delta}$ region.

The construction of a specially designed fixture for double-torsion testing has been completed. This special fixture assures good alignment of the loading system and soon will be used to test the double-torsion specimens under constant load condition.

Table I. Rapid Screening Test Data of NC-430

Specimen No.	Width B (mm)	Height W (mm)	Temperature T (°C)	Loading Rate $\dot{\delta}$ (in/min)	Peak Load Pmax (kg)	Apparent K_{IC} (MPa$\sqrt{m}$)
24A	2.023	4.971	RT	0.02	4.1	4.66
24B	2.024	4.972	RT	0.02	3.60	4.76
23B	2.021	4.963	RT	0.02	3.85	4.51
22B	2.018	4.971	RT	0.02	3.95	4.39
19B	1.991	4.972	1050	0.0002	4.87	5.41
7B	2.009	4.974	1050	0.02	4.63	5.16
21B	2.019	4.972	1050	0.02	4.10	4.66
15B	1.989	4.974	1350	0.0002	5.68	6.13
16B	1.983	4.972	1350	0.0002	6.74	7.32
18B	1.995	4.974	1350	0.002	5.47	6.01
17B	1.990	4.970	1350	0.02	4.97	5.37
20B	2.006	4.970	1350	0.02	4.15	4.72

NBS-5.12(B) - CRACK GROWTH MECHANISM MAPS

DISCUSSION OF CURRENT ACTIVITIES

Five notched specimens of KT-SiC were loaded under dead weight in four-point bend fashion for a constant applied stress intensity of 3.2 MPa$\sqrt{m}$. These tests were interrupted before failure at different durations. Table II lists the holding times and testing temperatures for these specimens. The apparent fracture toughness (K_{IC}) for this material (KT-SiC) has also been determined to be approximately 4.0 MPa$\sqrt{m}$.

These specimens are being polished and will be examined to see if any subcritical crack growth or cavitation took place.

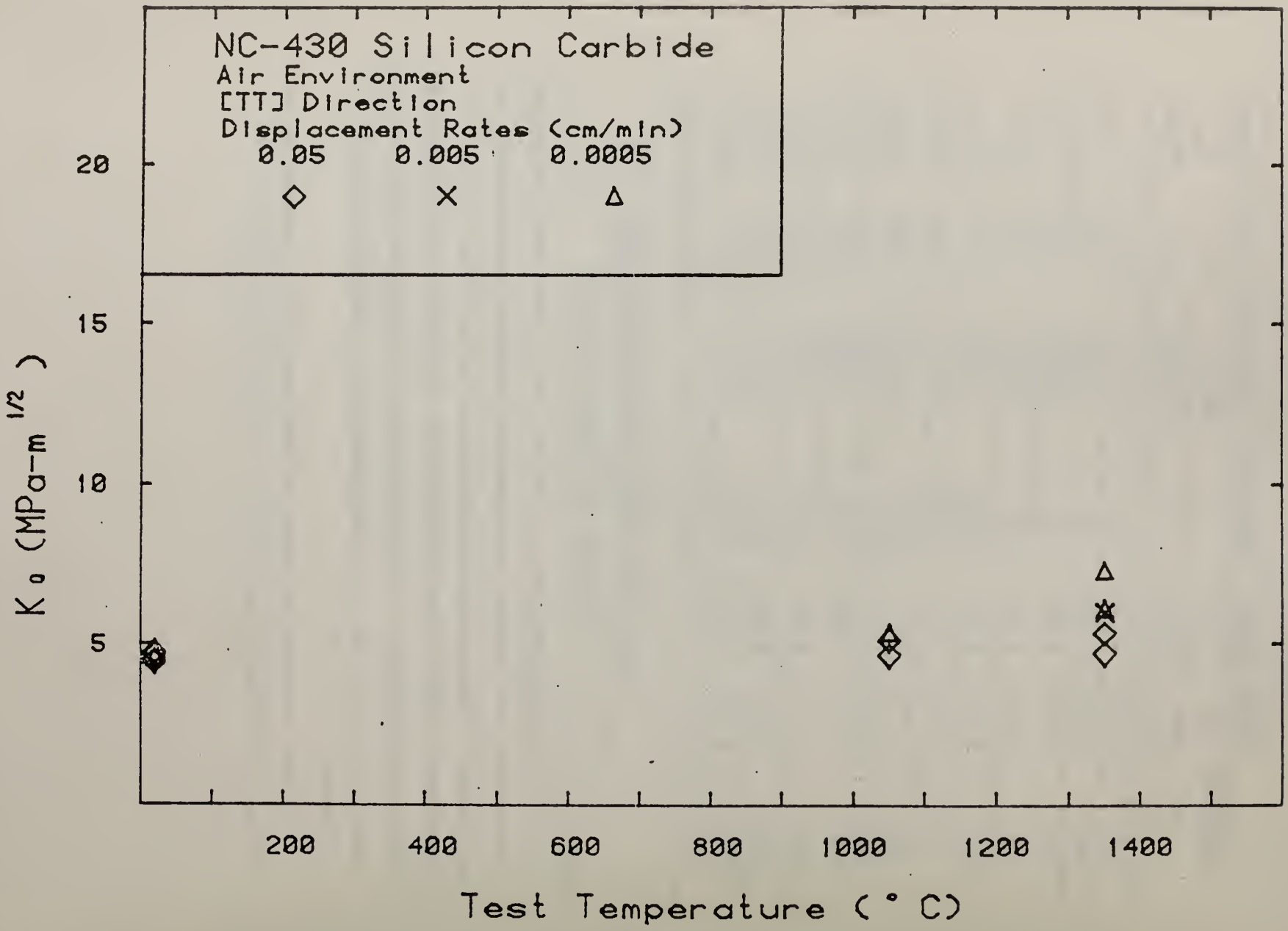

Figure 1. Plot of K_{IC} vs. T at different loading rates for NC-430.

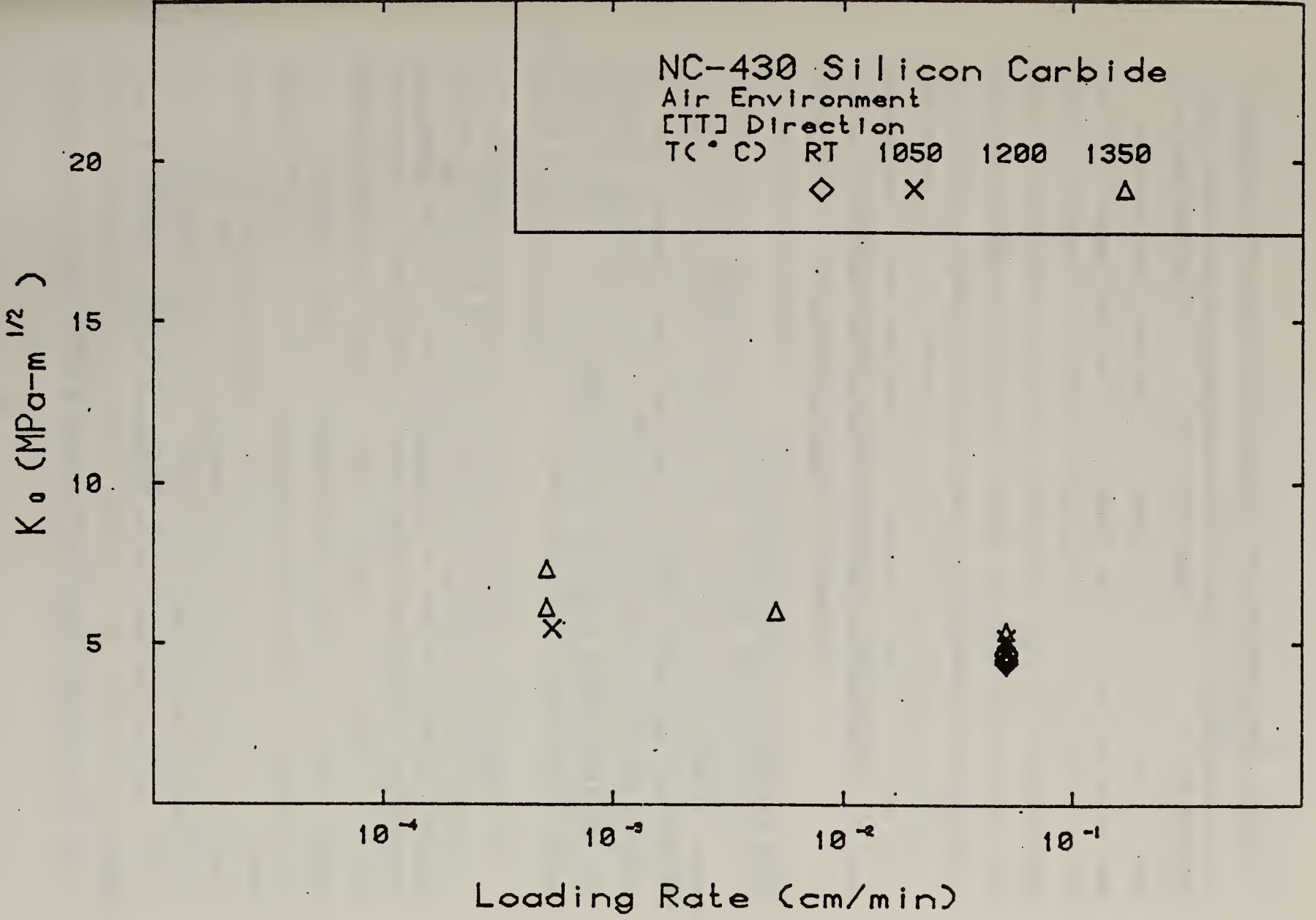

Figure 2. Plot of K_{IC} vs. $\dot{\delta}$ for NC-430 at various temperatures.

Table II. Test Durations and Temperatures for Creep Bending Test of KT-SiC (K = 3.2 MPa$\sqrt{m}$)

Specimen No.	Temperature (°C)	Duration (hr)
101	1300	95.5
102	1300	164.3
103	1300	65.0
104	1350	235.5
106	1350	66.0

NBS-5.12(C) - MICROSTRUCTURE AND PHASE ALTERATION

DISCUSSION OF CURRENT ACTIVITIES

Phase Analysis of As-Received Materials

X-ray diffraction data for samples of Carborundum silicon carbides--alpha-SiC and KT-SiC--and Norton silicon carbides--NC-203 and NC-430--were analyzed for SiC polytypes and impurity phases. The observed diffraction results, expressed as d-values (Å), were compared with reference values catalogued in the JCPDS card file. The indexed phases and polytypes of SiC contained in the file are listed in Table III.

Table III. JCPDS Indexed SiC Phases and Polytypes

Phase	Polytype	Card Number
α-SiC	2H	29-1126, 29-1130
α-SiC	4H	29-1127
α-SiC	6H	29-1128, 29-1131
α-SiC	15R	22-1301
α-SiC	21R	22-1319
α-SiC	33R	22-1316
α-SiC	51R	4-0756
β-SiC		29-1129

In addition, the cards for the indexed d-values for silicon (27-1402) and for a number of tungsten and aluminum carbides, oxycarbides, and oxides were used.

Because of the great structural similarity of all of the SiC polytypes and phases, a delineation of all of the polytypes and phase components of commercial silicon carbide materials is not possible. Moreover, analysis of a given material is complicated by compositional variations throughout the material and by preferred orientation of grains which can result, in the extremes, in abnormally large diffraction intensities or in absence of expected diffraction intensities. Nevertheless, it has been possible to obtain a "best fit" to one polytype and to presume the absence of some polytypes based on the absence of one or more characteristic diffraction peaks.

For all of the samples, the 6H polytype of α-SiC appears to be the dominant structural type. In most cases, except as noted below, it was not possible to distinguish β-SiC from the α-SiC's since possible β-diffraction peaks were obscured by the α-SiC peaks. The presence of important α-SiC peaks which were not associated with β-SiC indicated that the α-SiC's were the principal components of these materials. Minor amounts of α-SiC polytypes other than 6H will be discussed now for the specific materials.

1. Alpha-SiC: Alpha-SiC is a reaction bonded silicon carbide which contains no free silicon but presumably has Al and B incorporated in some form, since Al_2O_3 and B reportedly are used as sintering aids. In addition to the 6H polytype, a small amount of the 4H polytype appears to be present. The presence of other polytypes is doubtful. This material showed a number of weak diffraction peaks, particularly in the range $1.73\ \text{Å} < d < 1.78\ \text{Å}$, which suggest the presence of aluminum carbide and aluminum oxycarbide.

2. KT-SiC: This silicon carbide-based material is injection molded SiC, impregnated with free Si. The sample examined here was cut with the two examined surfaces transverse to the pressing direction. In addition to the 6H polytypes, small amounts of 2H, 4H, and 15R polytypes appear to be present in this material. The general agreement of ob-

served SiC diffraction intensities with the published values suggests that the SiC grains were not oriented with respect to the pressing direction.

This material was notable for the large amount of free silicon which appeared to be present. Moreover, the silicon distribution was highly variable, and the silicon grains appeared to be strongly oriented. The sample was examined at two positions on each of two opposite sides. The ratio, I_{Si}/I_{SiC}, of the major silicon peak to the major silicon carbide peak varied between one and three. Furthermore, the observed diffraction peaks for the free silicon showed enhanced diffraction by (111)-planes, and to a lesser extent, by (311)- and (511)-planes, indicating that these grains are oriented with their <111>-axis approximately parallel to the pressing direction.

3. NC-203: This is a hot-pressed silicon carbide which appears to contain minor amounts of 2H, 4H, and 15R polytypes and of β-SiC. Some weak to moderate diffraction peaks were observed which were assigned to WC. Evidence for other tungsten carbides was not found. A broad, weak diffraction peak at about d = 3.45 Å suggested the presence of a small amount of graphite, but since the position of the observed peak is shifted slightly from the expected position for the graphite diffraction peak (3.35 Å), this assignment is not certain.

4. NC-430: This siliconized silicon carbide material appears to be composed of 6H with perhaps a minor amount of β-SiC. The diffraction peaks for free silicon are not as strong as those for SiC (silicon content was estimated to be about 20 percent by volume based on x-ray data). The silicon distribution does not appear to be as variable or the silicon grains as highly oriented as in the case of KT-SiC.

Reactions of SiC in Gaseous Environments

The results reported here were obtained in conjunction with the work reported in Section (D) below. A sample of NC-203 and one of NC-430 were annealed at 1350 °C for four hours in the simulated coal-combustion

gas mixture (gas mixture A).* In addition, a fracture specimen of KT-SiC was examined.

As in previous investigations of the oxidation of silicon carbide materials in air, each of the specimens exhibited a peak or a composite peak in the range of 4.04 to 4.07 Å, which is evidence for an SiO_2 product phase--cristobalite or tridymite. The d-values for the product diffraction peaks are given in Table IV. Other than the assignment of the SiO_2-related peaks, the product phases have not been identified.

Previously obtained oxidation results for the air oxidation of NC-430 at 1400 °C for seven hours were re-examined. It was found that the major SiC diffraction peak, which is observed in the range of 2.515 to 2.519 Å for unoxidized samples, had split into two peaks, one at 2.512 Å and the other at 2.519 Å. This is apparently associated with a transformation of the polytypes.

*The gas was introduced at a rate of 500 ml/min with a nominal composition of 75% N_2, 11% CO_2, 7% O_2, 7% H_2O and an excess of + .1% SO_2.

Table IV. Diffraction d-Values for Product Phases on SiC Reacted in Combustion Gas Mixture A at 1350 °C for Four Hours; d-Values in Å

NC-203	NC-430	KT-SiC	Phase
6.32			
		4.15	
	4.10		
4.07	4.06		Low cristobalite or tridymite
		4.04	
4.01			
		3.74	
2.973			
		2.596	
2.238			
2.110			
		1.998	
		1.608	
1.581			
		1.443	
		1.357	
		1.245	
		1.108	
		0.960	

High-Temperature X-Ray Diffraction

Machining of the bonded ceramic fiber insulation and assembly of the x-ray diffraction furnace was completed. A second heating method was tested. This method uses a heater-sample holder which is machined from an SiC heating element. A test of a heating element in a test rig is shown in Figure 3. Although the heater performed satisfactorily, high contact resistances between the heater and the silicon carbide electrical power leads presented difficulties. An attempt to eliminate these resistances by coating the junctions with a mixture of Si and $MoSi_2$ powder, which then was arc-welded to form a bond, succeeded in reducing the resistance so that sufficient current could be passed through the heater to bring it to temperature. However, the welds tended to crack on cooling, and the $MoSi_2$ corroded the SiC. Subsequently, we have learned that it may be possible to form low resistance

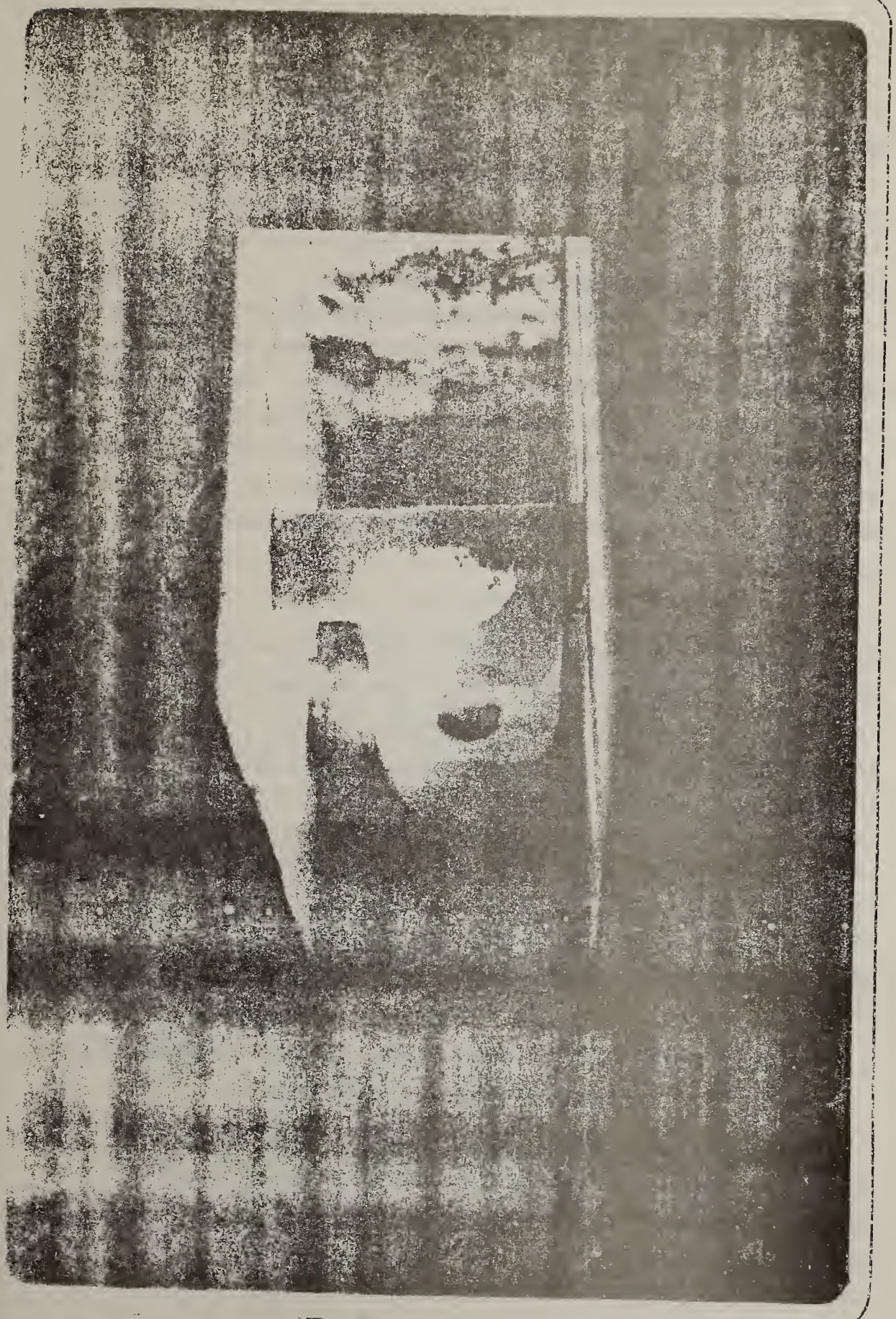

Figure 3. Test of silicon carbide heating element.

junctions by coating the junctions with Si powder only and heating in excess of 2000 °C.

A talk entitled, "High-Temperature X-Ray Diffraction and the Oxidation of Silicon Carbide", was given at the 85th Annual Meeting of the American Ceramic Society.

Models for Induced Microstresses and Microstrains

A general bulk material contains cracks and inclusions of varying sizes and placements. Towards the goal of describing mathematically the stress/strain states of a given material, a very idealized problem is under study as a first approximation. A thin slab of material containing a periodic array of cracks and inclusions can be discussed in terms of the solutions to the biharmonic equation if the regions of plasticity are ignored. Thus, a solution is being sought for the equation,

$$\nabla^2\nabla^2\Psi = 0,$$

for an infinite slab containing periodically placed extended elastic inclusions and nonplastic pores. While this problem is highly idealized, it has several useful and interesting features. First, the complex function formalism can be used along with the general solution techniques that are well discussed in the literature. Second, the interaction of the pores and inclusions can be studied. Third, the change in overall bulk properties, such as the compressibility, can be estimated. Fourth, the consequences of the differential thermal characteristics of the constituents can be estimated. And, fifth, it might be possible to consider plasticity in a subsequent perturbation treatment.

NBS-5.12(D) - MICROSTRUCTURE AND FRACTURE IN REACTIVE ENVIRONMENTS

DISCUSSION OF CURRENT ACTIVITIES

During the past quarter, we completed the construction of an apparatus for fracture testing of ceramic materials in controlled gaseous environments at elevated temperatures. Verification of the capabilities and operation of this apparatus was demonstrated with a set of initial fracture experiments on alpha silicon carbide in an

atmosphere of simulated combustion product gases. More controlled experiments, in terms of specimen orientation and machining, were then conducted on a siliconized silicon carbide material. These studies are described below.

Construction of an apparatus for fracture testing of selected structural ceramics in controlled gaseous environments at elevated temperatures was completed during the past quarter. The furnace for this apparatus is a commercially manufactured box furnace which we had specially designed. It is electrically heated with molybdenum disilicide heating elements and is capable of temperatures up to 1600 °C. The hot zone is approximately a 15 cm cube which is insulated with a refractory alumina. Load is transmitted into the hot-zone cavity by silicon carbide rods which are appropriately secured to special bellows assemblies attached to the top and bottom parts of the furnace. The test chamber, hot zone region and insulation, are enclosed in a gas tight steel jacket. Appropriate parts of this jacket and the furnace shell are water cooled, but in all cases the cooling water temperature is above the required dew point for the steam component of the gaseous atmosphere. The furnace is mounted in the frame of a gear driven universal testing machine. Typical load ranges are 100 to 500 N full scale with a 0.5 percent precision. Typical crosshead displacement rates range from 5 mm/min to 5×10^{-4} mm/min.

The test environment for this apparatus is a gaseous mixture of nitrogen, oxygen, steam, carbon dioxide and sulfur dioxide. The total pressure is nominally one atmosphere and the flow rate thorugh the furnace cavity is nominally 500 mL/min (STP). All the gaseous components except steam are supplied from tank gases with their flow rate and proportion established by mass flow controllers. A steam generator was constructed to generate the water vapor component of the gaseous environment. A thermostat bath is used to control both the steam partial pressure, via a condensor, and the temperature of the cooling water in the furnace shell and bellows assemblies to prevent water condensation in the furnace.

Having completed construction of the environmental testing apparatus, initial fracture experiments were begun on a miscellaneous collection of alpha silicon carbide specimens to verify operation of this system. Chevron-notched, four-point flexural specimens† (nominally, 2 x 5 x 50 mm) were used to determine the fracture toughness (K_{IC}) at temperatures of 1200 °C and 1500 °C. The gas composition for these measurements was 75 percent nitrogen, 7 percent oxygen, 11 percent carbon dioxide, 7 percent water vapor and 0.1% sulfur dioxide, which simulates the gaseous combustion products in an oxygen-rich fossil fuel system. Before the fracture test was conducted, the specimen was equilibrated at temperature and exposed to the flowing environment for four hours. The fracture tests were conducted at a constant displacement rate to failure, with both a high rate (0.5 mm/min) and a low rate (0.005 mm/min). The lower rate indicates the presence of subcritical crack growth and/or creep shielding at the crack tip. The fracture toughness was calculated using a variation of an analysis for chevron-notched specimens by D. G. Munz, J. L. Shannon, Jr., and R. T. Bubsey [Int. Journ. of Fracture 16, R137-R141 (1980)]. Using this analysis, the fracture toughness (K_{IC}) was determined from the maximum fracture load assuming that the crack went catastrophic at the minimum of the curve in stress intensity factor versus crack length. This assumption is only valid when subcritical crack growth is minimal. Accordingly, the values of K_{IC} at the rapid loading rate give a better measure of toughness and the values at the slower rates should be viewed as giving an indication of the extent of subcritical crack growth and/or creep blunting, giving lower values in the former case and higher values in the latter case.

---

†Material for these and subsequent tests was supplied in the form of square plate billets with nominal dimensions of 12 x 50 x 50 mm. (Most likely, these billets were cold pressed and sintered.) Two test orientations were used for the flexural specimens: a TP orientation and a TT orientation where T denotes a transverse direction and P denotes the plate direction. In both cases the crack propagated on a transverse (T) plane, but in the former case (TP orientation) the propagation direction was perpendicular to the plate (P), whereas in the latter case it was parallel to the plate (T).

Results of these fracture experiments for an alpha silicon carbide (HEXALLOY SA) are given in Table V. Comparison of these values with those measured in air, both here and in Task A, indicate that this environment has little synergetic influence with stress, as indicated by the fracture toughness. It, however, does not address any long term alterations in both microstructural and mechanical properties due to prolonged exposure. Having verified operation of the system with the miscellaneous alpha silicon carbide specimens, carefully machined and ground specimens of a siliconized silicon carbide (HEXALLOY KT) were tested using the same procedure. Results of these measurements are given in Table VI. There appears to be a slight effect of the environment in this case.

Table V. Critical Stress Intensity Factor (K_{IC}) for alpha-SiC (HEXALLOY SA)

Environment/ Temperature	Crack Orientation	Loading Rate/(mm/min)	K_{IC}/MPa•$m^{\frac{1}{2}}$
Air/25 °C	TP	0.5	7.8
	TT	0.5	6.1
	TT	0.005	6.3
Combustion Gas/ 1200 °C	TP	0.5	9.1
			10.6
	TP	0.005	9.3
			8.7
	TT	0.5	9.0
	TT	0.005	7.2
Combustion Gas/ 1500 °C	TT	0.5	6.1
	TT	0.005	5.7
	TT	0.001	5.3

[Combustion Gas: 75% N_2; 7% O_2; 11% CO_2; 7% H_2O; 0.1% SO_2]

Table VI. Critical Stress Intensity Factor (K_{IC}) for Siliconized SiC (HEXALLOY KT)

Environment/ Temperature	Crack Orientation	Loading Rate (mm/min)	K_{IC}/MPa·$m^{\frac{1}{2}}$
Combustion Gas/ 1050 °C	TT	0.5	6.1
		0.005	15.7
Combustion Gas/ 1200 °C	TT	0.5	12.7
	TT	0.005	22.8
Combustion Gas/ 1350 °C	TT	0.5	12.7
		0.005	18.5